Observational Study

Medicine®

OPEN

Prognostic biomarkers of cervical squamous cell carcinoma identified via plasma metabolomics

Huihui Zhou, PhD[a], Qi Li, MD, PhD[b,*], Tong Wang, PhD[a,*], Hong Liang, BM[a], Yanan Wang, PhD[a], Yani Duan, MM[a], Min Song, BM[b], Yaoxian Wang, MD, PhD[b], Hong Jin, MD, PhD[b]

Abstract

Cervical cancer is the second most common female malignancy worldwide. The metabolic profile of plasma associated with the prognosis of cervical cancer remains poorly understood. In this cross-sectional study, plasma samples were collected from three groups of patients with CSCC, namely primary patients before treatment (BT group), patients with a poor prognosis (PP group, including patients with distant metastasis and local recurrence), and patients with a good prognosis within two years after the first treatment (GP group). The plasma metabolomics was conducted to detect the dynamic changes of metabolites via ultra-performance liquid chromatography with quadrupole time-of-flight mass spectrometry. Multivariate analyses, including principle component, partial least square-discriminant, and orthogonal projection to latent structure-discriminant analyses, were performed to compare each pair of the three groups. The differential metabolites were identified by comparison of the exact m/z values and mass spectrometry (MS)/MS spectra with the structural information of the metabolites obtained from the Human Metabolome Database (http://www.hmdb.ca/) and LIPID MAPS (http://www.lipidmaps.org/). To screen for potential markers, receiver operating characteristic curve analysis of the differential metabolites. Finally, thirty plasma samples were collected from each group. Multivariate analyses showed that 31 metabolites were significantly different among the 3 groups studied. Of those, the 5 metabolites phosphatidyl choline (15:0/16:0), phosphatidyl glycerol (12:0/13:0), actosylceramide (d18:1/16:0), D-Maltose, and phthalic acid, with an area under the curve above 0.75, were identified as potential biomarkers. The present findings provide evidence for biomarkers to monitor prognosis of patients with CSCC, which may help in better managing the disease.

Abbreviations: AA = arachidonic acid, AUC = area under curve, BT = primary cervical cancer patients before treatment, $cPLA_2$ = cytosolic phospholipase A_2, CR = complete response, CSCC = cervical squamous cell carcinoma, ESI = electrospray ionization, FIGO = the International Federation of Gynecology and Obstetrics, GP = cervical cancer patients with good prognosis, LacCer = lactosylceramide, LPC = lysophosphatidylcholine, MBP = maltose-binding protein, OPLS-DA = orthogonal projection to latent structures discriminant analysis, PA = phthalic acid, PAE = phthalic acid ester, PC = phosphatidyl choline, PCA = principle component analysis, PG = phosphatidyl glycerol, PLS-DA = partial least squares-discriminant analysis, PP = cervical cancer patients with poor prognosis, QC = quality control, ROC = receiver operating characteristic, RT = retention time, SCC-Ag = squamous cell carcinoma antigen, SP = specificity, UPLC-Q-TOF/MS = ultra-performance liquid chromatography with quadrupole time-of-flight mass spectrometry, VIP = variable importance in the projection.

Keywords: biomarkers, cervical squamous cell carcinoma, plasma metabolomics, prognosis, UPLC-Q-TOF/MS

Editor: Hua Yang.

This study was supported by the National Natural Science Foundation of China (81372938, 81773368, and 81202154).

All procedures performed in this study involving human participants were in accordance with the ethical standards of the ethics committee at Harbin Medical University in Harbin, China and with the 1964 Helsinki declaration and its later amendments or comparable ethical standards. This article does not contain any studies with animals performed by any of the authors.

Informed consent was obtained from all individual participants included in the study.

Data availability: The metadata of metabolomics reported in this study is available via https://doi.org/10.6084/m9.figshare.7262195.v3.

The authors report no conflicts of interest.

Supplemental Digital Content is available for this article.

[a] *Chinese Center for Endemic Disease Control, Harbin Medical University,* [b] *Department of Gynecological Radiotherapy, Harbin Medical University Cancer Hospital, Harbin, P.R. China.*

[*] *Correspondence: Tong Wang, Chinese Center for Endemic Disease Control, Harbin Medical University, 157 Baojian Road, Harbin 150081, P.R. China (e-mail: wangtong@ems.hrbmu.edu.cn); Qi Li, Department of Gynecological Radiotherapy, Harbin Medical University Cancer Hospital, 150 Haping Road, Harbin 150081, P.R. China (e-mail: liqi@ems.hrbmu.edu.cn).*

Medicine (2019) 98:26(e16192)

Received: 27 November 2018 / Received in final form: 4 June 2019 / Accepted: 5 June 2019

http://dx.doi.org/10.1097/MD.0000000000016192

1. Introduction

Cervical cancer is the second most common female malignancy worldwide, with approximately 570,000 new cases and 311,000 deaths in 2018.[1] In China, cervical cancer is the second leading cause of cancer death among women, with over 102,000 new cases and 30,000 deaths recorded in 2014.[2] Although the mortality rates have recently declined owing to the promotion of early screening and development of the human papillomavirus vaccine,[3] cervical cancer continues to be a major public health problem. In developing countries, approximately two-thirds of patients are already at a locally advanced stage when diagnosed; their prognosis is poor, with a high risk of metastasis or relapse.[4] Therefore, it is necessary to explore biomarkers of cervical cancer to monitor better the outcome of these patients.

Metabolomics is a promising technology with a high sensitivity that can quantitatively measure the metabolite composition of a biological specimen. By identifying the metabolic profile, this methodology provides information that, otherwise, could not be obtained merely through other methodologies, such as proteomics and genomics. Metabolomics has been shown to have great potential for exploring biomarkers, particularly in malignant tumors, such as endometrial carcinoma, and breast and prostate cancers.[5–7] Metabolomics applications in cervical cancer have been mainly focused on diagnosis and treatment efficacy.[8,9] However, the metabolic profile of plasma associated with cervical cancer prognosis remains poorly understood. Therefore, we decided to explore plasma metabolomics to identify prognosis-related biomarkers of cervical squamous cell carcinoma (CSCC). The quest for useful and specific biomarkers that allow predicting outcomes will ultimately aid in developing appropriate and timely treatment strategies for those patients.

2. Materials and methods

2.1. Patients and study design

This cross-sectional study was approved by the ethics committee of Harbin Medical University in Harbin, China. Written informed consent was obtained from each patient before participation in the study. Data were collected was performed at the Department of Gynecological Radiotherapy, Harbin Medical University Cancer Hospital, between November 2016 and November 2017. Patients who met the following inclusion criteria were enrolled: diagnosis of CSCC (SCC histological subtype) confirmed by physical examination, histopathology, and imaging tests; evidence of primary CSCC before any treatment (BT group), and of CSCC with a poor prognosis (PP group; patients with local recurrence or distant metastasis confirmed by follow-up physical examination, and both blood and imaging tests), or with a good prognosis after the first treatment (GP group; patients without local recurrence, distant metastasis, and any other cancer-related discomfort within 2 years after the first treatment). The detailed demographic data, such as age and body mass index (BMI), and clinical characteristics, such as clinical stage and lymph node, were matched among the 3 groups. The exclusion criteria were: metabolic, liver, and kidney disease or any other cancer type, and missing clinical data. Disease staging was based on the International Federation of Gynecology and Obstetrics (FIGO) system.

2.2. Plasma samples

When the patients were diagnosed by the clinicians and met the inclusion criteria, the blood samples were collected. All patients were required to fast and avoid medication and alcohol for 12 hours. 5 mL of whole blood was then collected into a heparin sodium anticoagulation tube. Fresh blood was centrifuged at 3000 rpm/min for 10 minutes at room temperature, and the supernatant, corresponding to the plasma sample, was collected and stored at –80 °C until analysis.

2.3. Quality control samples

To ensure the stability and repeatability of the ultra-performance liquid chromatography with the quadrupole time-of-flight mass spectrometry (UPLC-Q-TOF/MS) system, quality control (QC) samples were prepared by mixing equal volumes of different individual plasma and used in both electrospray ionization positive (ESI+) and negative (ESI-) modes. One QC sample was run after every 9 test samples.

2.4. Sample pretreatment

After thawing the plasma sample at room temperature, 80 μL were transferred into a 1.5 mL centrifuge tube and mixed with 10 μL of internal standard (0.3 mg/ml; L-2-chlorophenylalanine) by vortexing 10 s. Subsequently, 240 μL of the protein precipitation [methanol/acetonitrile (1:1, v/v)] were added, and the mixture was vortexed again for 1 minute. The mixture was then ultrasound extracted on an ice water bath for 10 minutes and allowed to stand at –20 °C for 30 minutes. After centrifugation for 15 minutes at 4 °C, 200 μL of the supernatant were transferred into an LC vial and stored at –80 °C until injection analysis.

2.5. Chromatography

A 5 μL pretreated sample was injected into a 2.1 × 100 mm (1.7 μm) ACQUITY UPLC BEH C18 column (Waters, Milford, CT) using the ACQUITY UPLC system (Waters, Milford, CT). The mobile phase was a mixture of water containing 0.1% (v/v) formic acid (A) and acetonitrile with 0.1% (v/v) formic acid (B). The elution gradient was as follows: 5% to 20% B for 0 to 2 minutes; 20% to 60% B for 2% to 4 minutes; 60% to 100% B for 4 to 11 minutes; 100% B for 11 to 13 minutes; and 5% B for 13 to 13.5 minutes and then for additional 13.5 to 14.5 minutes. The mobile phase flow rate was 0.40 mL/min at 45 °C.

2.6. Mass spectrometry

MS was performed using an AB Triple TOF 5600 (AB Sciex, Boston, MA) equipped in both ESI+ and ESI- modes. The ion spray voltage was set at 5.5 kV for the ESI+ mode and at 4.5 kV for the ESI- mode. The ion source temperature was set 550 °C and the centroid data were collected in full scan mode from 70 m/z to 1000 m/z.

2.7. Data preprocessing

The raw data files were imported to Progenesis QI software (Waters, Milford, CT) for preprocessing. After baseline filtering, peak identification, integration, retention time (RT) correction, peak alignment, and normalization, a matrix of features including the RT, m/z values, and peak area was produced.

Table 1

Demographic and clinical characteristics of the enrolled patients.

Characteristics	BT	PP	GP	*P* value
Number of subjects	30	30	30	
Age (mean ± SD)	52.20 ± 7.99	53.27 ± 8.55	52.40 ± 8.02	.92
BMI (mean ± SD)	24.98 ± 4.09	23.95 ± 2.54	25.11 ± 2.77	.24
Marry Age (mean ± SD)	22.46 ± 2.95	22.52 ± 2.80	24.21 ± 4.17	.20
Pregnancy times (mean ± SD)	2.90 ± 1.52	3.24 ± 1.55	2.63 ± 1.52	.32
Births times (mean ± SD)	1.50 ± 0.90	1.55 ± 0.74	1.27 ± 1.05	.44
Abortion times (mean ± SD)	1.40 ± 1.35	1.69 ± 1.47	1.37 ± 1.27	.61
Primiparous age (mean ± SD)	23.52 ± 2.71	23.45 ± 2.87	24.19 ± 2.77	.56
Menopause (Yes/No)	14/16	13/17	17/13	.56
Heart disease (Yes/No)	2/28	0/30	0/30	.33
Hypertension (Yes/No)	4/26	2/28	0/30	.16
FIGO Stage				.08
I	0	5	4	
II	18	16	21	
III	12	9	5	
First treatment regimen				.58
Surgery	–	11	9	
Chemoradiotherapy	–	19	21	
Response evaluation				.44
CR	–	15	12	
PR	–	15	18	
Lymphatic metastasis (Yes/No)	12/18	14/16	–	.40
SCC-Ag (mean ± SD)	12.83 ± 15.31	5.81 ± 10.94	0.89 ± 0.83	<.001
Hemoglobin (mean ± SD)	118.73 ± 23.02	119.92 ± 11.27	127.46 ± 9.97	.08

BMI = body mass index, BT = primary cervical cancer patients before treatment, CR = complete response, FIGO = the International Federation of Gynecology and Obstetrics, GP = cervical cancer patients with good prognosis, PP = cervical cancer patients with poor prognosis, PR = partial response, SCC-Ag = squamous cell carcinoma antigen, SD = standard deviation.

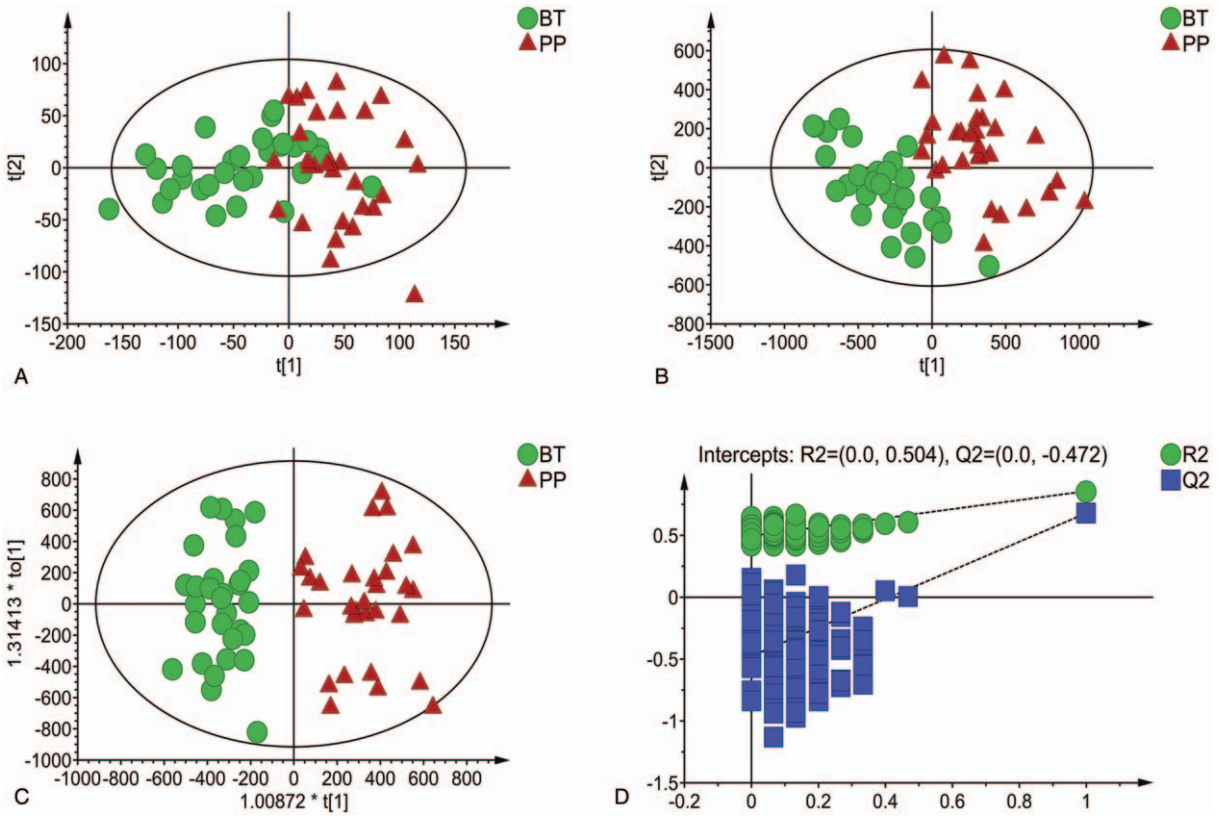

Figure 1. Multivariate analysis for cervical squamous cell carcinoma samples from primary patients before treatment and from those with poor prognosis after the first treatment. (A) Principle component analysis score plot ($R2X_{cum}$ = 0.630, $Q2_{cum}$ = 0.388); (B) Partial least squares-discriminant analysis score plot ($R2Y_{cum}$ = 0.784, $Q2_{cum}$ = 0.620); (C) Orthogonal projection to latent structures discriminant analysis score plot ($R2Y_{cum}$ = 0.856, $Q2_{cum}$ = 0.680); (D) Validation plot (R2 = 0.504; Q2 = −0.472).

2.8. Statistical analyses

After preprocessing, the matrix was imported into SIMCA software (Umetrics, Umeå, Sweden). Unsupervised principle component analysis (PCA) was used to visualize the overall distribution of the samples and evaluate the stability of the analysis process. Then, the supervised partial least squares-discriminant analysis (PLS-DA) and orthogonal projection to latent structures discriminant analysis (OPLS-DA) were performed to determine the global metabolic differences between each pair of groups. Corresponding variable importance in the projection (VIP) values were calculated in the OPLS-DA model. The 7-round cross-validation and 200 response permutation tests were conducted to evaluate the quality of the model to prevent overfitting.

2.9. Biomarker identification and selection

The differential metabolites that were selected based on the criteria of VIP >1 and $P < .05$, were then identified by comparison of the exact m/z values and MS/MS spectra using the structural information of the metabolites from both the Human Metabolome Database (http://www.hmdb.ca/) and LIPID MAPS (http://www.lipidmaps.org/). Receiver operating characteristic (ROC) analysis was performed using MetaboAnalyst 4.0 to screen for differential metabolites with an area under the curve (AUC) of above 0.75 as potential markers. The levels of potential markers in the 3 groups were plotted in an error bar chart to visualize metabolite changes.

3. Results

3.1. Characteristics of the enrolled patients

The detailed demographic and clinical characteristics of the patients included in this study are listed in Table 1. Thirty plasma samples were collected from each patient group. Regarding FIGO stage, 18 patients in the BT group had stage II disease and 12 had stage III. In the PP group, 5, 16, and 9 patients had stage I, II, and III disease, respectively, which corresponded to 4, 21, and 5 patients in the GP group. There were no statistical differences observed in patients' age, body mass index, status of marriage and childbirth, menopause, heart disease, hypertension, disease stage, and hemoglobin level among the 3 groups ($P > .05$). The first treatment regimen of patients in the PP and GP groups were mainly surgery and chemoradiotherapy, and there was no significant difference in the 2 groups. According to the response evaluation criteria in solid tumors (RECST, version 1.1), 15 in the PP group were diagnosed as complete response (CR) and 15 as PR after the first treatment regimen; 12 and 18 patients in the GP group were diagnosed as CR and PR respectively. The levels of SCC antigen (SCC-Ag) of the patients in the BT, PP, and GP groups were significantly different ($P < .001$) corresponding to the median ± standard deviation of 12.83 ± 15.31, 5.81 ± 10.94, and 0.89 ± 0.83, respectively.

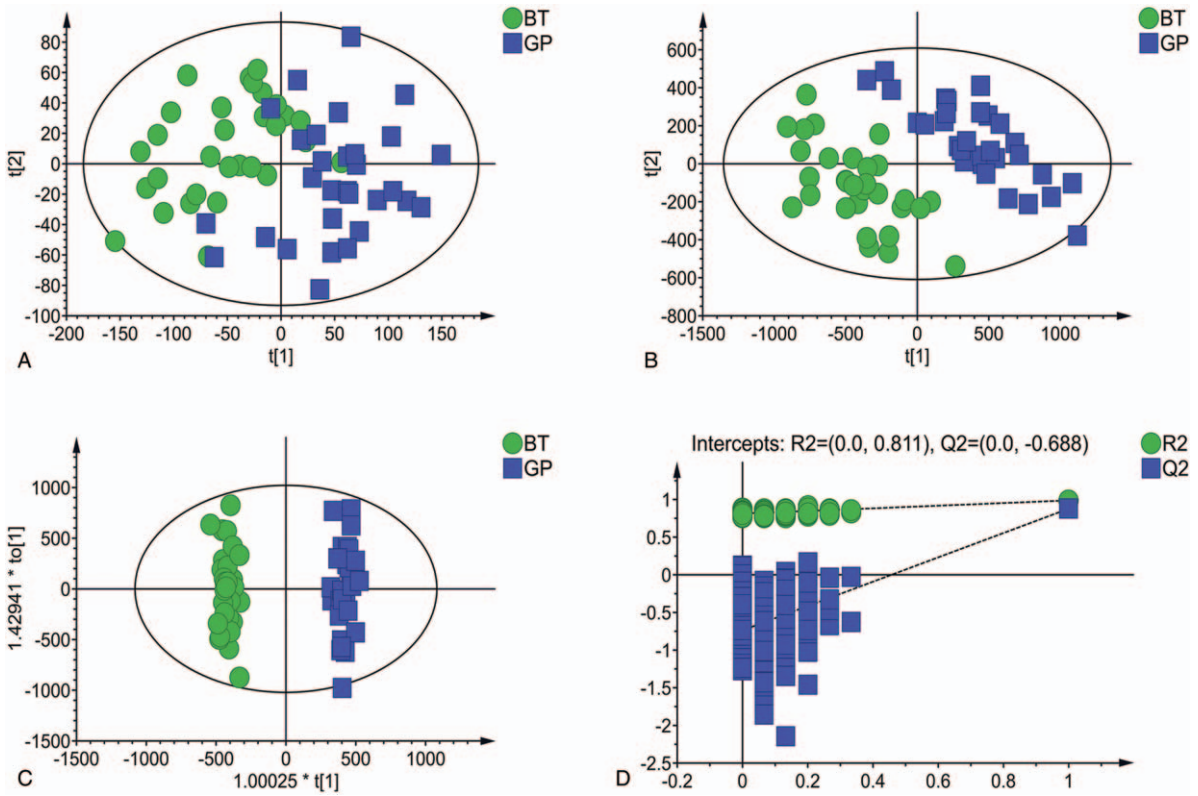

Figure 2. Multivariate analysis for cervical squamous cell carcinoma samples from primary patients before treatment and from those with good prognosis after the first treatment. (A) Principle component analysis score plot ($R2X_{cum} = 0.591$, $Q2_{cum} = 0.409$); (B) Partial least squares-discriminant analysis score plot ($R2Y_{cum} = 0.865$, $Q2_{cum} = 0.790$); (C) Orthogonal projection to latent structures discriminant analysis score plot ($R2Y_{cum} = 0.988$, $Q2_{cum} = 0.878$); (D) Validation plot ($R2 = 0.811$; $Q2 = -0.688$).

3.2. Metabolic profiles of the 3 groups

The typical chromatograms (Figure S1, Supplemental Content, http://links.lww.com/MD/D64 which illustrates the overall metabolic profiles) showed that all plasma samples had a strong instrumental analysis signal, large peak capacity, and good reproducibility of RT. After preprocessing, the final dataset consisted of 7959 ions in the ESI+ mode and 10,915 ions in the ESI- mode. PCA revealed that the QC samples were densely clustered (Figure S2, Supplemental Content, http://links.lww.com/MD/D64 which illustrates the distribution of all samples), indicating that the results of the metabolic analysis were reliable.

3.3. Metabolic profiles of BT group versus PP group

The unsupervised PCA method detected the differentiation between the BT and PP groups to some extent, but the trend was not obvious (Fig. 1a). The supervised methods of PLS-DA and OPLS-DA were performed, and the prediction models were established. As shown in the PLS-DA (2 parameters: R2Y = 0.784 and Q2 = 0.620) and OPLS-DA (2 parameters: R2Y = 0.856 and Q2 = 0.680) score plots, the samples of the BT and PP groups were clearly divided into 2 categories (Fig. 1b, c). The validation plot obtained from 200 permutation tests, as shown in Figure 1d, showed that all permuted R2 and Q2 values on the left were lower than the original point on the right, and that the Q2 regression line (in blue) had a negative intercept, indicating that the model prevented overfitting and was both stable and reliable. According to the VIP >1 and $P < .05$ criteria, 258 differential metabolites were identified between the 2 groups. The heat map for these metabolites showed distinct segregation (Figure S3, Supplemental Content, http://links.lww.com/MD/D64 which illustrates the result of the cluster analysis for BT group vs PP group).

3.4. Metabolic profiles of BT group versus GP group

The PCA, PLS-DA, and OPLS-DA score plots revealed significant differences between the BT and GP groups (Fig. 2a, b, and c); the validation tests showed the reliability of the OPLS-DA model (Fig. 2d). A total of 228 metabolites were found important in the sample classification, as indicated by the criteria of VIP >1 and $P < .05$. Moreover, the heat map for these metabolites showed distinct segregation (Figure S4, Supplemental Content, http://links.lww.com/MD/D64 which illustrates the result of the cluster analysis for BT group vs GP group).

3.5. Metabolic profiles of GP group versus PP group

There was a certain overlap of the plasma samples between the GP and PP groups in the PCA score plot (Fig. 3a). However, the supervised methods of PLS-DA and OPLS-DA showed clear separations between the 2 groups (Fig. 3b, c). The validation tests revealed that the OPLS-DA model was reliable (Fig. 3d). Based on the same criteria as before (VIP >1 and $P < .05$), 174 differential metabolites were identified in the 2 groups, and the corresponding heat map showed distinct segregation (Figure S4,

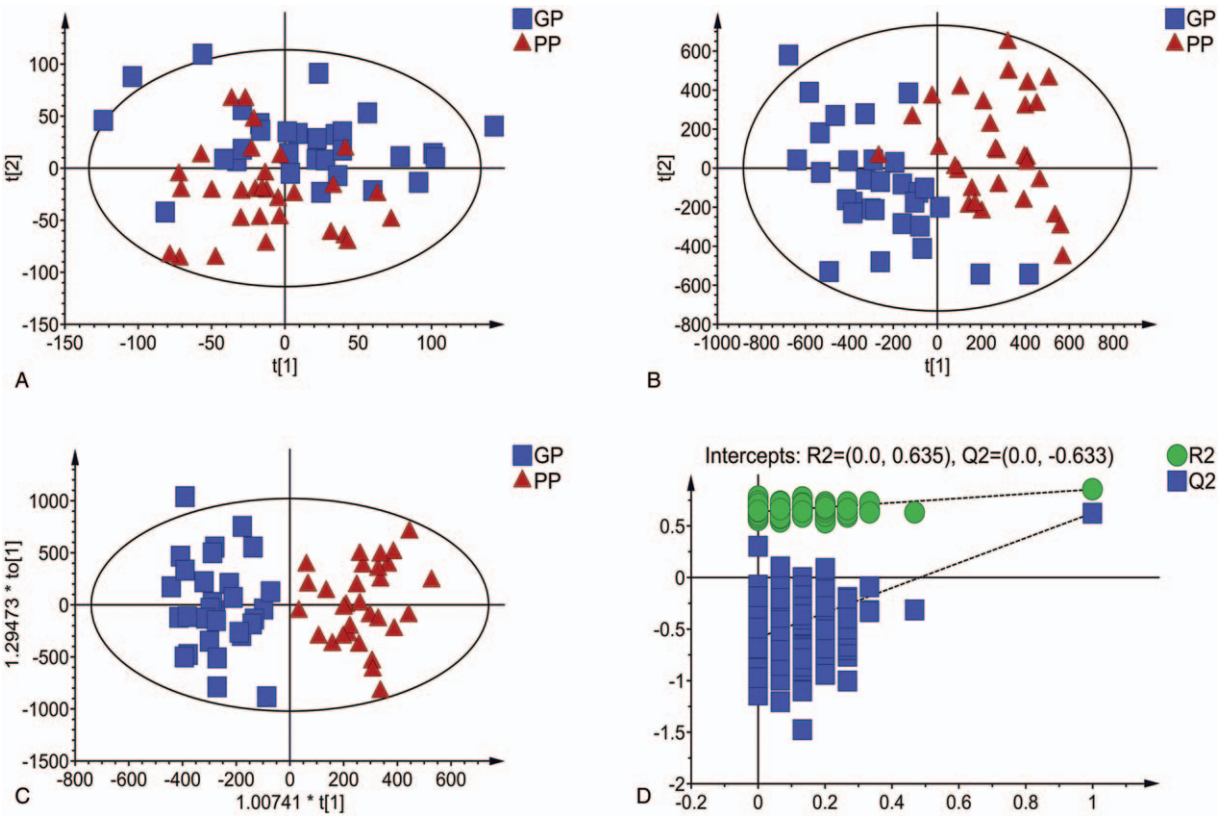

Figure 3. Multivariate analysis for cervical squamous cell carcinoma samples from patients with good and poor prognoses after the first treatment. (A) Principle component analysis score plot ($R2X_{cum} = 0.568$, $Q2_{cum} = 0.360$); (B) Partial least squares-discriminant analysis score plot ($R2Y_{cum} = 0.818$, $Q2_{cum} = 0.623$); (C) Orthogonal projection to latent structures discriminant analysis score plot ($R2Y_{cum} = 0.853$, $Q2_{cum} = 0.624$); (D) Validation plot (R2 = 0.635; Q2 = −0.633).

Supplemental Content, http://links.lww.com/MD/D64 which illustrates the result of the cluster analysis for GP group vs PP group).

3.6. Screening of differential metabolites between groups

A total of 31 metabolites were significantly different among BT, PP, and PP groups (Fig. 4), including glycerophospholipid, sphingomyelin, and glycosphingolipid. The detailed statistical information of these metabolites is listed in Table 2. The results of the ROC analysis showed that the AUCs of 5 specific metabolites, namely phosphatidyl choline [PC (15:0/16:0)], phosphatidyl glycerol [PG (12:0/13:0)], lactosylceramide [LacCer (d18:1/16:0)], D-Maltose, and phthalic acid (PA), were above 0.75. These values of AUC, as well as the sensitivity (SE) and specificity (SP) associated with these metabolites are summarized in Table 3; the combined AUCs were 0.97 (BT vs PP), 0.97 (BT vs GP), and 0.91 (GT vs PP), respectively. The trends in the levels observed for the 5 metabolites among the 3 groups are shown in Figure 5. The levels of PA, D-Maltose, and PG (12:0/13:0) were highest in BT group, followed by PP group, and finally GP group. The level of LacCer (d18:1/16:0) was also highest in the group, but decreased in GP group PP group. The level of PC (15:0/16:0) was highest in GP group and lowest in PP group.

4. Discussion

The demographic and clinical characteristics of the patients enrolled were evenly distributed among the groups, with the exception of SCC-Ag, which is a tumor marker of CSCC with presumable prognostic value.[10,11] However, previous studies showed that the SE and SP of SCC-Ag are relatively low. Moreover, there is a lag associated with the diagnosis, enabling SCC-Ag to meet fully clinical requirements.[10,11]

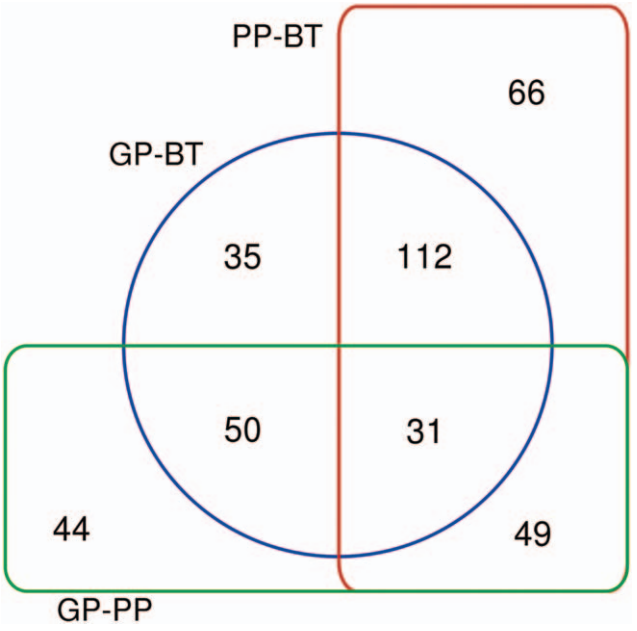

Figure 4. Venn diagram of metabolites identified by multiple comparisons between the 3 groups: primary patients before treatment (BT group), patients with poor (PP group) and good (GP group) prognoses after the first treatment. The red frame shows 258 differential metabolites identified by BT and PP groups comparison; the blue frame shows 228 differential metabolites identified on comparing the BT and GP groups; the green frame shows 174 differential metabolites identified by GP and PP groups comparison.

In this study, we analyzed the plasma samples of patients from each BT, PP, and GP group. We investigated the metabolic profiles of the collected samples by UPLC-Q-TOF/MS and developed multivariate analysis models between the groups studied. The results revealed significant differences in the plasma metabolism among the CSCC patients associated with different prognoses. Five metabolites, namely PC (15:0/16:0), PG (12:0/13:0), LacCer (d18:1/16:0), D-Maltose, and PA, were identified as potential biomarkers for predicting outcomes and monitoring prognosis of patients with CSCC, as their combined AUCs were sufficient to distinguish the subjects among the 3 groups.

Recent studies on cancer metabolomics showed that the lipid metabolism plays an important role in tumor development.[12,13] Phospholipids are a key component of the cell membrane and one of the most widely distributed bioactive substances in the body. They participate in metabolic processes and signal transduction pathways.[14] The main biological functions of PC (15:0/16:0) include storing energy, protecting the liver, increasing high-density lipoprotein levels, and restoring vascular elasticity. Endogenous PC can produce arachidonic acid (AA) and lysophosphatidylcholine (LPC) through deacylation promoted by the cytosolic phospholipase A_2 ($cPLA_2$).[15] Previous studies showed that AA and its downstream mediators have a role in promoting tumor cell proliferation, invasion, and metastasis.[16,17] Lysophosphatidic acid produced from LPC by lysophospholipase D also plays an important role in promoting cell proliferation.[18,19] In this study, the level of PC (15:0/16:0) was highest in the GP group, followed by BT and PP. This may be because endogenous PC in patients with primary and recurrent CSCC is converted to AA and LPC by $cPLA_2$, resulting in the decrease of the PC level itself. We anticipate that this reaction would be inhibited in patients with a good prognosis.

We found that the level of PG (12:0/13:0) was highest in the BT group, followed by PP and GP. PG is a small molecular phospholipid; it primarily exists in the cell membrane and is essential for the synthesis of cardiolipin.[20] Recent studies revealed that eukaryotic mitochondria contain 2 independent pools of PG, which are mainly distributed in the phospholipid bimolecular structure of the inner and outer membranes of the mitochondria.[21] At physiological concentrations of cardiolipins, the accumulation of PG lead to the disintegration of the mitochondrial outer membrane, thus affecting mitochondrial morphology and function, and this mitochondrial dysfunction often exists in tumor cells.[22,23]

In this study, the LacCer (d18:1/16:0) level was highest in the BT group, followed by GP and being lowest in PP. It was shown that LacCer is specific and highly expressed in cell lines of breast cancer, but it is not related to recurrence;[24] these findings are similar to ours. LacCer synthase is activated by pro-inflammatory factors to generate LacCer, which in turn activates "oxygen-sensitive" signaling pathways that affect cellular processes, such as proliferation, migration, and angiogenesis. Dysfunctions in these pathways can affect tumor development and metastases.[25] However, the reason why LacCer (d18:1/16:0) level does not increase in patients with recurrence remains to be elucidated.

Regarding the level of maltose, it was highest in the BT group, followed by PP and GP; this trend might be associated with tumor formation and recurrence. Due to the lack of maltase activity in the blood, maltose is mainly transported to the kidney by the

Table 2

Detailed information on the 31 potential biomarkers found significant between the 3 groups.

				BT vs PP			BT vs GP			GP vs PP		
Metabolites	m/z	RT (min)	Mass Error (ppm)	VIP	*P*	FC1	VIP	*P*	FC2	VIP	*P*	FC3
SM (d18:0/16:0)	749.58	10.03	0.46	2.81	.00	0.76	1.26	.02	1.14	5.14	.00	0.67
PE (20:0/22:5 (4Z,7Z,10Z,13Z,16Z))	820.59	10.10	0.14	1.48	.01	1.24	1.87	.00	1.49	1.58	.04	0.83
PC (18:0/20:4 (5Z,8Z,11Z,14Z))	854.59	10.13	1.08	12.21	.01	1.13	16.21	.00	1.27	14.74	.02	0.89
PC (15:0/16:0)	718.54	10.29	0.51	1.06	.00	0.86	1.05	.00	1.15	2.97	.00	0.75
PC (16:0/16:0)	778.56	10.29	1.51	3.14	.00	0.85	1.44	.04	1.07	6.41	.00	0.79
SM (d18:1/18:0)	775.60	10.47	1.01	2.62	.03	0.89	2.21	.03	1.15	6.93	.00	0.77
PE (16:1 (9Z)/24:1 (15Z))	844.61	10.78	1.02	1.64	.00	0.77	1.08	.00	1.24	2.98	.00	0.62
PC (14:0/20:0)	806.59	11.20	0.98	1.69	.00	0.76	1.34	.00	1.28	3.81	.00	0.59
13,17-Dimethylpentatetracontane	678.78	11.37	−0.48	1.52	.01	0.97	1.94	.00	0.95	1.60	.01	1.02
SM (d18:2/21:0)	769.62	11.46	1.13	3.69	.00	0.67	2.52	.00	1.39	6.61	.00	0.48
SM (d16:1/24:1)	829.65	11.46	1.32	7.93	.00	0.68	4.38	.00	1.29	12.97	.00	0.53
8-Hydroxyguanine	185.08	2.01	−1.17	1.89	.00	0.91	2.33	.00	0.84	1.77	.00	1.08
Desmosdumotin C	335.12	5.06	−1.80	1.56	.00	0.96	1.72	.00	0.94	1.18	.00	1.02
Phthalic acid	149.02	5.22	−2.50	1.55	.00	0.94	1.96	.00	0.90	1.64	.00	1.05
LysoPC (18:3 (6Z,9Z,12Z))	562.31	5.76	−1.44	2.50	.00	2.01	1.00	.02	1.41	2.19	.04	1.43
DAT (16:0/23:0 (2Me[S],3OH[S],4Me[S],6Me[S]))	992.76	8.40	0.16	2.48	.01	0.95	3.49	.00	0.90	3.03	.01	1.05
Dichotellate A	441.30	8.44	1.78	1.48	.00	0.97	1.71	.00	0.95	1.02	.01	1.02
D-Maltose	365.10	8.52	−1.72	1.40	.00	0.94	1.97	.00	0.88	1.82	.00	1.06
PC (18:2 (9Z,12Z)/22:6 (4Z,7Z,10Z,13Z,16Z,19Z))	874.56	8.95	1.05	1.99	.00	1.32	2.42	.00	1.53	1.40	.03	0.86
SM (d18:2/15:0)	685.53	9.16	0.73	2.89	.00	1.14	4.47	.00	1.32	4.07	.00	0.87
SM (d16:1/18:1)	745.55	9.16	1.13	4.07	.01	1.10	6.13	.00	1.23	5.04	.01	0.90
PC (14:0/20:3 (5Z,8Z,11Z))	756.55	9.26	−0.53	6.10	.00	1.62	3.04	.00	1.36	3.34	.05	1.19
PC (15:0/22:5 (4Z,7Z,10Z,13Z,16Z))	792.56	9.48	1.17	2.42	.00	1.18	3.54	.00	1.39	3.13	.00	0.85
LacCer (d18:1/16:0)	906.62	9.48	1.01	3.26	.00	0.37	1.89	.00	0.59	1.70	.00	0.63
LacCer (d18:1/16:0)	884.61	9.49	0.51	4.15	.00	0.44	2.54	.00	0.60	1.59	.00	0.73
PC (15:0/20:4 (5Z,8Z,11Z,14Z))	766.54	9.50	1.31	5.64	.00	1.14	6.77	.00	1.28	5.89	.02	0.89
PC (18:0/22:6 (4Z,7Z,10Z,13Z,16Z,19Z))	878.59	9.53	−0.74	1.35	.04	1.14	2.05	.00	1.31	1.45	.03	0.87
PG (12:0/13:0)	607.40	9.76	2.24	1.15	.00	0.91	1.43	.00	0.84	1.10	.00	1.08
PE (20:0/22:6 (4Z,7Z,10Z,13Z,16Z,19Z))	818.57	9.86	−0.15	3.48	.00	1.20	4.23	.00	1.38	4.05	.02	0.86
PE (20:4 (5Z,8Z,11Z,14Z)/P-16:0)	722.51	9.91	0.84	4.64	.00	0.75	2.86	.02	1.27	10.25	.00	0.59
PS (P-16:0/22:6 (4Z,7Z,10Z,13Z,16Z,19Z))	790.50	9.91	−1.96	3.70	.00	0.71	1.71	.04	1.23	7.22	.00	0.57

BT = primary cervical cancer patients before treatment, FC = fold change, GP = cervical cancer patients with good prognosis, LacCer = lactosylceramide, LysoPC = lysophosphatidylcholine, PC = phosphatidyl choline, PE = phosphatidyl ethanolamine, PG = phosphatidyl glycerol, PP = cervical cancer patients with poor prognosis, PS = phosphatidyl serine, RT = retention time, SM = sphingmyelin, VIP = variable importance in the projection.

Table 3

AUC, SE, and SP of 5 biomarkers and the combination of these biomarkers in 3 groups.

	BT vs PP			BT vs GP			GP vs PP		
Metabolites	AUC	SE	SP	AUC	SE	SP	AUC	SE	SP
Phthalic acid	0.91	0.83	0.80	1.00	1.00	0.97	0.82	0.73	0.80
D-Maltose	0.76	0.63	0.93	0.99	0.97	0.97	0.82	0.77	0.80
PG (12:0/13:0)	0.79	0.67	0.83	0.98	0.90	1.00	0.76	0.60	0.90
LacCer (d18:1/16:0)	0.98	0.93	0.97	0.90	0.87	0.77	0.79	0.80	0.70
PC (15:0/16:0)	0.78	0.77	0.80	0.78	0.67	0.77	0.90	0.87	0.87
Combination	0.97	0.94	0.87	0.97	0.92	0.89	0.91	0.86	0.80

AUC = area under curve, BT = primary cervical cancer patients before treatment, GP = cervical cancer patients with good prognosis, LacCer = lactosylceramide, PC = phosphatidyl choline, PG = phosphatidyl glycerol, PP = cervical cancer patients with poor prognosis, SE = sensitivity, SP = specificity.

maltose-binding protein (MBP), where it is hydrolyzed to glucose by maltase to be reabsorbed into the body.[26,27] MBP also plays a significant role in enhancing immune function and promoting apoptosis.[28,29] According to our findings, we hypothesized the MBP and its metabolic pathways are inhibited in tumor cells, thus affecting the transport of maltose. Meanwhile, the apoptosis promoted by MBP might have been inhibited, resulting in a decline of the immune function.

Phthalic acid esters (PAEs), as common environmental endocrine disruptors, can enter the body through the respiratory system and skin, interfering with the endocrine system. Additionally, PA is a PAE metabolite with mutagenicity and carcinogenicity potential.[30] In agreement, we observed that PA had the highest level in the BT group, followed by PP, and being lowest in GP. This trend also suggests that PA promotes the development of CSCC.

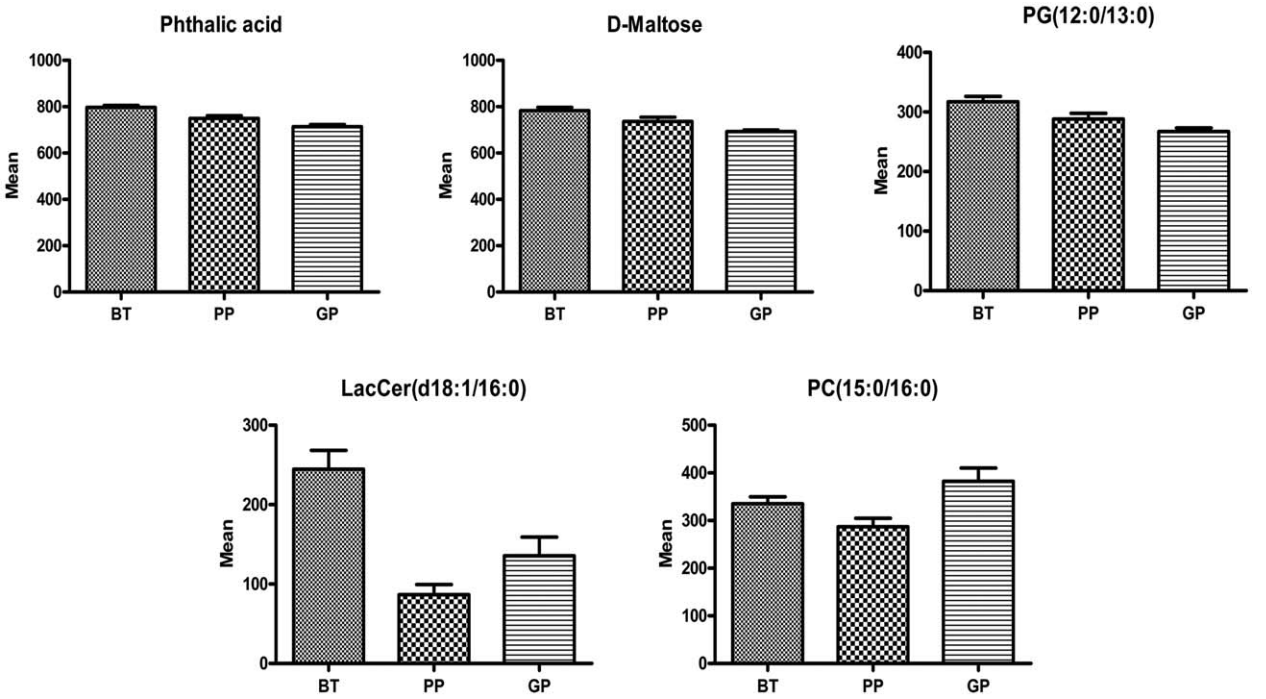

Figure 5. Error bar chart (Mean ± 95% confidence interval) demonstrating dynamic changes in the 5 biomarkers of the 3 groups.

4.1. Strengths and limitations

This is the first study to examine the differences in the plasma metabolic profiles of CSCC patients with different prognoses. After controlling for any influencing factors of the biological samples, we identified 5 plasma metabolites that differed significantly between the patients. However, this study presents several limitations. First, the cross-sectional design is not ideal for assessing the causal relationship between prognosis and metabolites. Second, our sample size was small, which might have affected our results despite adjustment for influencing factors. Therefore, prospective studies with larger sample sizes are needed to confirm the predictive value of the 5 metabolites identified.

5. Conclusion

The plasma metabolites PC (15:0/16:0), PG (12:0/13:0), LacCer (d18:1/16:0), D-Maltose, and PA were significantly different in patients with CSCC exhibiting different prognoses. Therefore, these 5 metabolites may be considered as potential prognostic biomarkers. As a consequence, our study may ultimately lead to the improvement of treatment strategies resulting in a better management of patients with CSCC.

Acknowledgments

The authors would like to express their sincere gratitude to all doctors and nurses who participated in recruiting participants and collecting samples. We are grateful to all participants involved in this study.

Author contributions

Conceptualization: Huihui Zhou, Qi Li, Tong Wang.
Data curation: Huihui Zhou.
Formal analysis: Huihui Zhou.
Funding acquisition: Qi Li, Tong Wang.
Investigation: Huihui Zhou, Qi Li, Hong Liang, Yanan Wang, Yani Duan, Min Song, Yaoxian Wang, Hong Jin.
Resources: Qi Li, Min Song, Yaoxian Wang, Hong Jin.
Supervision: Qi Li, Tong Wang.
Writing – original draft: Huihui Zhou.
Writing – review & editing: Qi Li, Tong Wang.
Tong Wang orcid: 0000-0002-8619-2650.

References

[1] Bray F, Ferlay J, Soerjomataram I, et al. Global cancer statistics 2018: GLOBOCAN estimates of incidence and mortality worldwide for 36 cancers in 185 countries. CA Cancer J Clin 2018;68:394–424.
[2] Chen WQ, Sun KX, Zheng RS, et al. Report of cancer incidence and mortality in different areas of China, 2014 [in Chinese]. China Cancer 2018;27:1–4.
[3] Ginsburg O, Bray F, Coleman MP, et al. The global burden of women's cancers: a grand challenge in global health. Lancet 2017;389:847–60.
[4] Bazaz M, Shahry P, Latifi SM, et al. Cervical cancer literacy in women of reproductive age and its related factors. J Cancer Educ 2017;2017:1–8.
[5] McCartney A, Vignoli A, Biganzoli L, et al. Metabolomics in breast cancer: a decade in review. Cancer Treat Rev 2018;67:88–96.
[6] Shi K, Wang Q, Su Y, et al. Identification and functional analyses of differentially expressed metabolites in early stage endometrial carcinoma. Cancer Sci 2018;109:1032–43.
[7] Kaushik AK, Vareed SK, Basu S, et al. Metabolomic profiling identifies biochemical pathways associated with castration-resistant prostate cancer. J Proteome Res 2014;13:1088–100.
[8] Walker H, Burrell M, Flatley J, et al. A metabolite profiling method for diagnosis of precancerous cervical lesions and HPV persistence. Bioanalysis 2017;9:601–8.
[9] Hou Y, Yin M, Sun F, et al. A metabolomics approach for predicting the response to neoadjuvant chemotherapy in cervical cancer patients. Mol Biosyst 2014;10:2126–33.
[10] Chan YM, Ng TY, Ngan HY, et al. Monitoring of serum squamous cell carcinoma antigen levels in invasive cervical cancer: is it cost-effective. Gynecol Oncol 2002;84:7–11.

[11] Oh J, Bae JY. Optimal cutoff level of serum squamous cell carcinoma antigen to detect recurrent cervical squamous cell carcinoma during post-treatment surveillance. Obstet Gynecol Sci 2018;61:337–43.
[12] Hashmi S, Wang Y, Suman DS, et al. Human cancer: is it linked to dysfunctional lipid metabolism. Biochim Biophys Acta 2015;1850: 352–64.
[13] Huang C, Freter C. Lipid metabolism, apoptosis and cancer therapy. Int J Mol Sci 2015;16:924–49.
[14] Fahy E, Cotter D, Sud M, et al. Lipid classification, structures and tools. Biochim Biophys Acta 2011;1811:637–47.
[15] You JC, Yang J, Fang RP, et al. Analysis of phosphatidylcholines (PCs) and Lysophosphatidylcholines (Lyso PCs) in Metastasis of Breast Cancer Cells [in Chinese]. Prog Biochem Biophys 2015;42:563–73.
[16] Benesch MG, Ko YM, McMullen TP, et al. Autotaxin in the crosshairs: taking aim at cancer and other inflammatory conditions. FEBS Lett 2014;588:2712–27.
[17] Nimptsch A, Pyttel S, Paasch U, et al. A MALDI MS investigation of the lysophosphatidylcholine/phosphatidylcholine ratio in human spermatozoa and erythrocytes as a useful fertility marker. Lipids 2014;49: 287–93.
[18] Leblanc R, Peyruchaud O. New insights into the autotaxin/LPA axis in cancer development and metastasis. Exp Cell Res 2015;333:183–9.
[19] Llona-Minguez S, Ghassemian A, Helleday T. Lysophosphatidic acid receptor (LPAR) modulators: the current pharmacological toolbox. Prog Lipid Res 2015;58:51–75.
[20] Jiang F, Rizavi HS, Greenberg ML. Cardiolipin is not essential for the growth of Saccharomyces cerevisiae on fermentable or non-fermentable carbon sources. Mol Microbiol 1997;26:481–91.
[21] Pokorna L, Cermakova P, Horvath A, et al. Specific degradation of phosphatidylglycerol is necessary for proper mitochondrial morphology and function. Biochim Biophys Acta 2016;1857:34–45.
[22] Calvert AE, Chalastanis A, Wu Y, et al. Cancer-associated IDH1 promotes growth and resistance to targeted therapies in the absence of mutation. Cell Rep 2017;19:1858–73.
[23] Suhaili SH, Karimian H, Stellato M, et al. Mitochondrial outer membrane permeabilization: a focus on the role of mitochondrial membrane structural organization. Biophys Rev 2017;9:443–57.
[24] Zhu T, Xu L, Xu X, et al. Analysis of breast cancer-associated glycosphingolipids using electrospray ionization-linear ion trap quadrupole mass spectrometry. Carbohydr Res 2015;402:189–99.
[25] Chatterjee S, Pandey A. The Yin and Yang of lactosylceramide metabolism: implications in cell function. Biochim Biophys Acta 2008;1780:370–82.
[26] Lina BA, Jonker D, Kozianowski G. Isomaltulose (Palatinose): a review of biological and toxicological studies. Food Chem Toxicol 2002;40:1375–81.
[27] Tahara Y, Fukuda M, Yamamoto Y, et al. Metabolism of intravenously administered maltose in renal tubules in humans. Am J Clin Nutr 1990;52:689–93.
[28] Fernandez S, Palmer DR, Simmons M, et al. Potential role for Toll-like receptor 4 in mediating Escherichia coli maltose-binding protein activation of dendritic cells. Infect Immun 2007;75:1359–63.
[29] Zhang Q, Ni W, Zhao X, et al. Synergistic antitumor effects of Escherichia coli maltose binding protein and Bacillus Calmette-Guerin in a mouse lung carcinoma model. Immunol Lett 2011;136:108–13.
[30] Bang DY, Lee IK, Lee BM. Toxicological characterization of phthalic acid. Toxicol Res 2011;27:191–203.